INSTRUMENTS AND EXPERIMENTAL TECHNIQUES, 2025, No. 1

GENERAL EXPERIMENTAL TECHNIQUE

ROTATION OF THE PLANE OF POLARIZATION OF OPTICAL RADIATION CAUSED BY THE ADDITION OF TWO ELLIPTICALLY POLARIZED WAVES CONTROLLED BY SOUND

© 2025 V. M. Kotov*

Institute of Radio Engineering and Electronics named after V.A. Kotelnikov

Russian Academy of Sciences Russia, Fryazino, Moscow region

e-mail: vmk277@ire216.msk.su

Received July 01, 2024

Revised September 19, 2024

Accepted September 26, 2024

Abstract. A method for controlled rotation of the plane of polarization of linearly polarized radiation is proposed, based on the addition of two mutually orthogonal elliptically polarized waves, the parameters of which are controlled by a sound wave in the process of acousto-optic (AO) Bragg diffraction. It is shown theoretically that the angle of polarization rotation depends on the ellipticity of the beams and does not depend on the wavelength of light. The maximum polarization rotation is determined by the ellipticity of the summed waves and can reach approximately 45º. Experiments on controlling the polarization rotation of optical radiation with a wavelength of 0.63 μm, performed on the basis of an AO cell made of a paratellurite crystal, confirmed the main theoretical conclusions.

DOI: 10.31857/S00328162250113e3

1. INTRODUCTION

Acousto-optic (AO) cells allow control of many parameters of optical radiation: its amplitude, phase, frequency, direction of light propagation, etc. [1, 2]. Currently, the development of AO cells is developing in two directions - improving old ones that have proven themselves in practice AO elements, such as deflectors [3–5], modulators [6], etc., and the creation of fundamentally new devices, for example, combiners of optical beams with both the same [7] and different [8] wavelengths, meters of energy-geometric parameters of laser radiation [9], meters of the temperature distribution of micro-objects [10], AO elements for controlling many beams simultaneously [11], AO

delay lines for measuring the characteristics of external influences [12], filtering of spatial frequencies of two-color radiation [13], etc.

Among all AO devices, a special place is occupied by devices that use the diffraction of two natural modes of a crystal on a single acoustic wave. These devices include AO-splitters [14], AO-modulators of radiation with arbitrary polarization [15, 16], image analyzers [17], etc. This paper describes another application of AO-diffraction of two natural modes of a crystal on a single acoustic wave, which allows for controlled rotation of the polarization plane of linearly polarized radiation by changing the frequency of the acoustic wave. The effect is based on the addition of two mutually orthogonal elliptically polarized waves, the amplitudes and phases of which are controlled by the frequency of the sound wave during AO-interaction. This significantly expands the range of tasks that can be solved using AO-devices. Such devices are in demand, for example, in laser Doppler anemometry, where the efficiency of light scattering significantly depends on polarization [18], in various interferometers to obtain maximum contrast interference patterns [19], in laser gyroscopes, etc.

2. THEORY

Let us first define the conditions under which the addition of two mutually orthogonal elliptically polarized waves leads to the formation of a linearly polarized wave. Let the waves propagate along some direction z, and the projections of the electric induction vectors $\mathbf{D}_1$ and $\mathbf{D}_2$ on the directions x and y, orthogonal to each other and orthogonal to z, are determined by the relations [20]

$$D_{x1}=a_1\cos(\omega t+\delta_m),\ D_{y1}=a_2\sin(\omega t+\delta_m), \quad (1)$$

$$D_{x2}=b_1\sin(\omega t);\ D_{y2}=b_2\cos(\omega t).$$

Here D_{x1}, D_{y1} and D_{x2}, D_{y2} are projections of vectors $\mathbf{D}_1$ and $\mathbf{D}_2$ in the directions x and y; a_1, a_2 are amplitudes of projections of the 1st ellipse; b_1, b_2 are amplitudes of projections of the 2nd ellipse; ω is the cyclic frequency, t is time; δ_m is the phase difference between oscillations of the 1st and 2nd ellipses. It is assumed that $a_2/a_1 = b_1/b_2 = \rho$, where ρ is the ellipticity of the superimposed waves. The projection of the resulting wave in the direction x is given by the formula

$$D_{x1} + D_{x2} = a_1\cos(\omega t+\delta_m) + b_1\sin(\omega t) = T_1\cos(\omega t + \delta_1), \quad (2)$$

where

$$T_1=\sqrt{\left(a_1\cos\delta_m\right)^2+\left(-a_1\sin\delta_m+b_1\right)^2}\,, \qquad (3)$$

$$\mathrm{tg}\delta_1=\frac{a_1\sin\delta_m-b_1}{a_1\cos\delta_m}. \qquad (4)$$

Similarly, the resulting wave along the direction y is found:

$$D_{y1}+D_{y2}=a_2\sin(\omega t+\delta_m)+b_2\cos(\omega t)=T_2\cos(\omega t+\delta_2). \qquad (5)$$

Here

$$T_2=\sqrt{\left(a_2\cos\delta_m\right)^2+\left(a_2\sin\delta_m+b_2\right)^2}\,, \qquad (6)$$

$$\mathrm{tg}\delta_2=-\frac{a_2\cos\delta_m}{a_2\sin\delta_m+b_2}. \qquad (7)$$

The resulting ellipse is formed as the result of combining two harmonic oscillations directed along the axes x and y . The semi-axes a and b of the resulting ellipse are given by the formulas [20, 21]

$$a^2=\frac{1}{2}\left(T_1^2+T_2^2+\sqrt{\left(T_1^2+T_2^2\right)-4T_1^2T_2^2\sin^2\delta}\right), \qquad (8)$$

$$b^2=\frac{1}{2}\left(T_1^2+T_2^2-\sqrt{\left(T_1^2+T_2^2\right)-4T_1^2T_2^2\sin^2\delta}\right). \qquad (9)$$

Here a is the major semi-axis, b is the minor semi-axis; $\delta=\delta_2-\delta_1$. The angle ψ of inclination of the major semi-axis is related to T_1 , T_2 and δ by the relationship [20]

$$\mathrm{tg}2\psi=\frac{2T_1T_2}{T_1^2-T_2^2}\cos\delta\,. \qquad (10).$$

Note that the cyclic frequency ω does not appear in expressions (8)–(10), which means that the semi-axes a , b and the phase δ do not explicitly depend on the wavelength of light λ.

The condition for linear polarization of the resulting ellipse is defined as the minor semi-axis of the ellipse being equal to zero: $b = 0$. In this case, the inclination of the polarization vector will be equal to the angle ψ. Expression (9) at $b = 0$, $T_1 \neq 0$, $T_2 \neq 0$ leads to the relation $\sin\delta = 0$, i.e. $\delta = n\,\pi$, where n is an integer. From this, it follows that $\mathrm{tg}\,\delta = 0$. Using the relation $\mathrm{tg}\,\delta = \mathrm{tg}\,(\delta_2-\delta_1) = (\mathrm{tg}\,\delta_2 - \mathrm{tg}\,\delta_1)\,/\,(1+\mathrm{tg}\,\delta_2\,\mathrm{tg}\,\delta_1)$, we get $\mathrm{tg}\,\delta_2 = \mathrm{tg}\,\delta_1$.

Then from formulas (4) and (7), the following relation is derived:

$$\frac{a_1\sin\delta_m-b_1}{a_1\cos\delta_m}=-\frac{a_2\cos\delta_m}{a_2\sin\delta_m+b_2}, \qquad (11)$$

from which

$$\sin\delta_m=\frac{a_1a_2-b_1b_2}{a_2b_1-a_1b_2}. \qquad (12)$$

This equation determines the phase shift δ_m between the added ellipses depending on the amplitudes of the ellipses a_1, a_2, b_1, b_2 under the condition that the total radiation will be linearly polarized.

For practical application of the obtained results, let's connect the amplitudes a_1, a_2, b_1, b_2 with additional conditions. Let's assume that the amplitude of one of the ellipses increases, while the other decreases, but in such a way that the total intensity of the beams remains constant. For this, we define the amplitudes in the following form:

$$a_1=A\sqrt{0.5(1+P)},\quad a_2=\rho A\sqrt{0.5(1+P)},\quad b_1=\rho A\sqrt{0.5(1-P)},\quad b_2=A\sqrt{0.5(1-P)}. \quad (13)$$

Here A is the effective amplitude of the beams, ρ is the ellipticity, P is a parameter that determines the ratio of amplitudes. It is assumed that all parameters are positive, with $\rho \le 1$. When choosing amplitudes in the form (13), the total intensity of the added beams will be the same for any values of P, namely, it will be given by the relation

$$a_1^2+a_2^2+b_1^2+b_2^2=A^2\left(1+\rho^2\right).$$

After substituting expressions (13) into formula (12), we get

$$\sin\delta_m=-\frac{2\rho P}{\left(1-\rho^2\right)\sqrt{1-P^2}}. \quad (14)$$

Figure 1 shows the dependencies of phase change δ_m on parameter P for different values of ρ, equal to 0.9, 0.8, 0.7, 0.6, and 0.5 (curves *1 – 5* respectively). It can be seen that as ρ decreases, the slope of the dependencies of δ_m on P becomes less steep. Analysis shows that parameter P, increasing from zero, cannot exceed approximately (1-ρ). Otherwise, $\sin\delta_m \ge 1$.

Fig. 1. Dependence of phase change δ_m on parameter P for ellipticity values of 0.9, 0.8, 0.7, 0.6, 0.5, corresponding to curves *1 – 5*.

Figure 2 shows the dependencies of the angle ψ of polarization plane inclination, calculated according to formula (10) under the condition $\delta = 0$ and fulfilling relations (13), which are used to calculate T_1 and T_2 according to expressions (3) and (6). Here, curves *1 – 5* correspond to the same ellipticities as the curves in Fig. 1. It can be seen that here also the slope of the curves decreases with decreasing ellipticity. The range of angle ψ change is approximately 45° at $\rho = 0.9$ and approximately 30° at $\rho = 0.5$.

Fig. 2. Dependence of the rotation angle ψ of the total polarization vector on parameter P. Curves *1 – 5* correspond to the same ellipticities as the curves in Fig. 1.

The change in amplitudes of elliptically polarized waves and the phase change between waves can be implemented through Bragg AO-diffraction.

Figure 3 shows the vector diagram of AO-diffraction, which is proposed for performing such a task. It is assumed that diffraction occurs in a uniaxial gyrotropic crystal TeO_2. The wave vector surfaces of "extraordinary" and "ordinary" rays are denoted by numbers *1* and *2*. In the figure, the direction *z* coincides with the optical axis of the crystal, and *x* is the direction orthogonal to the optical axis. The optical face *S*, on which the initial optical radiation with wave vector **K** is incident, is oriented at an angle α to the *x* axis. The radiation splits in the crystal into two eigenwaves with elliptical polarization $\mathbf{K}_1$ and $\mathbf{K}_2$, belonging to wave surfaces 1 and 2 respectively. A transverse acoustic wave with wave vector **q**, oriented at an angle β to the direction *x*, propagates in the crystal. Note that the vector **q** is directed almost "tangentially" to wave surface 2, which ensures the smallest deviation of the end of the wave vector **q** from wave surface 2 with a significant change in the length of vector **q** (a mode similar to the operation mode of an AO-deflector [2]). This point is especially important since it is assumed to control the parameters of optical waves within a wide range of sound frequency changes. To analyze the polarization rotation effect, let's assume that the polarization of the incident wave **K** coincides with the polarization of the wave $\mathbf{K}_1$, i.e., all radiation inside the crystal is concentrated in the wave $\mathbf{K}_1$. This wave, as a result of anisotropic AO-diffraction on the acoustic wave **q**, diffracts in the direction of wave $\mathbf{K}_3$, belonging to surface 2. In the overmodulation mode, all radiation contained in the wave $\mathbf{K}_3$ returns again to the wave $\mathbf{K}_1$, but part of the radiation diffracts into the wave $\mathbf{K}_2$ as a result of isotropic diffraction. Diffraction into two closely located orders is possible; it is carried out on the "side" lobes of the radiation from the acoustic transducer [22]. Thus, as a result of "reverse" diffraction, two eigenwaves with elliptical polarization $\mathbf{K}_1$ and $\mathbf{K}_2$ are formed, the amplitudes of which vary depending on the diffraction conditions. In other words, a controlled "transfer" of energy from wave $\mathbf{K}_1$ to $\mathbf{K}_2$ occurs. Note that in this case, isotropic diffraction is considered as an important component of output optical radiation formation. The efficiency of isotropic diffraction in TeO_2 on the "slow" acoustic wave, observed in experiments, is quite high. It is only twice less than the efficiency of anisotropic diffraction [2]. This is quite sufficient to form, in our case, eigenwaves $\mathbf{K}_1$ and $\mathbf{K}_2$ with comparable amplitudes.

Fig. 3. Vector diagram of AO-diffraction in a uniaxial gyrotropic crystal.

The phase shift between eigenwaves is due to the nature of AO-interaction. In papers [23, 24], the phase shift caused by the sound wave was theoretically and experimentally investigated. It is shown there that the phase shift of radiation participating in diffraction can reach approximately 360º relative

to the phase of radiation that has not diffracted on the acoustic wave. Strictly speaking, in beams participating in AO-diffraction, a phase shift is always present. This follows from the fact that the amplitudes of all orders formed during AO-interaction are complex, which means the presence of a phase shift.

3. EXPERIMENT

The effect of optical radiation polarization plane rotation was observed in experiments where the polarization rotation was performed using an AO-cell made of TeO_2. The source of optical radiation was a He-Ne laser generating light at a wavelength of 0.63 μm. The dimensions of the crystal from which the AO-cell was made were $1.3\times1.0\times1.5$ cm^3 along the crystallographic axes [110] , $[1\bar{1}0]$ and [001] respectively, where [001] is the optical axis of the crystal *z*, [110] is the direction *x* (Fig. 3). The optical face of the crystal was "beveled" at an angle $\alpha = 8.3^\circ$ relative to the (001) plane, the acoustic face - at an angle $\beta = 3.7^\circ$ relative to the (110) plane. The acoustic wave was generated by a piezoelectric transducer made of $LiNbO_3$ and cold-welded to TeO_2 using the cold welding method [25]. The dimensions of the transducer are 0.3×0.3 cm^2. The transducer generated a transverse acoustic wave in the frequency range of 25-50 MHz. The speed of sound in the crystal was $0.63\cdot10^5$ cm/s.

Figure 4 shows a photograph of the manufactured AO cell. Here *1* is the microwave input, through which a high-frequency electrical signal is supplied to the cell; *2* is a paratellurite crystal TeO_2, which is the main element of the cell; *3* is the crystal holder; *4* is a heat sink located on the side of the piezoelectric transducer. It is necessary to dissipate heat from the cell, as the cell operates in overmodulation mode, i.e., at increased electrical power, which leads to heating of the cell. In the experiments, the voltage of the electrical signal was approximately 10 V, which corresponds to about 1 W of electrical power on a 50 Ohm load. Note that the heat sink provided stable cell operation for 2-3 hours.

Fig. 4. Photograph of the experimental AO cell.

Rotation of the polarization plane was accomplished by changing the frequency of the signal supplied to the cell. The process of measuring the polarization plane rotation was as follows: initially, a signal with a frequency of 36 MHz was applied to the AO cell. The cell was oriented in such a way that radiation with the maximum possible intensity and minimum ellipticity was formed at its output. The ellipticity of the radiation was controlled by a polarizer located at the output of the cell. The light intensity was measured by a photodetector positioned behind the polarizer. At each frequency value,

the polarizer was oriented in positions of minimum and maximum light transmission. The rotation angle was determined by the position of minimum transmission of the polarizer, as the angular orientation of the polarizer is most sensitive to the minimum radiation transmission. The wave ellipticity was defined as the ratio of signals measured in positions of minimum and maximum transmission. The signal at maximum transmission was approximately 600 mV across the entire sound frequency measurement range. During the measurements, only the sound frequency was changed, while the generator power and the orientation of the AO cell remained unchanged. Figure 5 shows the experimental results for the polarization rotation angle ψ, determined by the minimum signal, displayed as circles connected by an interpolation curve (solid line, left ordinate scale), depending on the sound frequency *f*. The same figure shows the ellipticity values of the rays as triangles (right ordinate scale). The dashed curve is an interpolation of the obtained results. It can be seen that the dependence of angle ψ on f is generally non-linear. This result is quite expected, since, as shown in [24], the dependence of the optical beam phase shift on the sound frequency during AO interaction is non-linear. In the dependence of ψ on *f*, two sections with frequency ranges of 36-43 MHz and 45-50 MHz can be distinguished, in each of which the dependencies are practically linear. They can be used in practice for linear control of polarization rotation by changing the sound frequency. Figure 5 shows that the ellipticity of the output beams does not exceed 0.07. This is quite acceptable for many practical applications.

Fig. 5. Dependence of the angle ψ of polarization plane rotation (solid curve, left ordinate scale) and ellipticity ρ (dashed curve, right scale) on the frequency *f* of the sound wave.

It is necessary to add the following: the range of variation of the angle ψ obtained from theoretical calculations does not exceed approximately 45º (see Fig. 2), while the similar range of angles obtained in experiments reaches approximately 50º (Fig. 5). This discrepancy can be explained by the fact that during the experiments, the condition of strict linearity of the output polarization was not met, and in the region where even slight ellipticity exists, the range of angles ψ can be significantly exceeded.

4. CONCLUSIONS

Based on the above, the following conclusions can be drawn.

1. A method for controlled rotation of the polarization plane of linearly polarized radiation is proposed, based on the addition of two mutually orthogonal elliptically polarized waves. It is revealed that the total radiation will be linearly polarized when condition (12) is satisfied.

2. To control the amplitudes and phases of waves, it is proposed to use the features of Bragg AO diffraction - diffraction on the side "lobes" of the acoustic transducer radiation, as well as the phase shift of optical beams due to the nature of AO interaction.

3. Experiments on controlled change of the polarization plane rotation angle of optical radiation with a wavelength of 0.63 μm, performed on an AO cell made of paratellurite crystal, confirmed the main theoretical conclusions: polarization rotation by an angle of about 50º was obtained when the sound frequency changed from 36 to 50 MHz. The ellipticity of the output radiation did not exceed 0.07.

FUNDING

The work was carried out within the framework of the state assignment of Kotelnikov Institute of Radio Engineering and Electronics of RAS
No. 075-00395-24-03.

REFERENCES

1. *Magdich L.N., Molchanov V.Ya.* Acousto-optical devices and their applications Moscow: Sov. Radio, 1978.
2. *Balakshiy V.I., Parygin V.N., Chirkov L.E.* Physical foundations of acousto-optics. Moscow: Radio i svyaz, 1985.
3. *Antonov S.N.* // PTE. 2019. No. 3. P. 89. https://doi.org/ 10.1134/S0032816219020174
4. *Antonov S.N.* // PTE. 2019. No. 6. P. 82. https://doi.org/ 10.1134/S0032816219060016
5. *Antonov S.N., Rezvov Yu.G.* // PTE. 2021. No. 5. P.100. https://doi.org/ 10.31857/S0032816221040017
6. *Antonov S.N., Rezvov Yu.G.* // PTE. 2021. No. 5. P.105. https://doi.org/ 10.31857/S0032816221050025
7. *Antonov S.N.* // PTE. 2021. No. 4. P. 51. https://doi.org/ 10.31857/S0032816221030162
8. *Kotov V.M.* // PTE. 2023. No. 3. P. 61. https://doi.org/ 10.31857/S0032816223020222
9. *Gasanov A.R., Gasanov R.A., Akhmedov R.A., Agaev E.A*. // PTE. 2020. No. 2. P. 109. https://doi.org/ 10.31857/S0032816220020111

10. *Machikhin A.S., Batshev V.I. Zinin P.V., Shurygin A.V., Khokhlov D.D., Pozhar V.E., Martyanov P.S., Bykov A.A., Boritko S.V., Troyan I.A., Kazakov V.A.* // PTE. 2017. No. 3. P.100. https://doi.org/ 10.7868/S0032816217020100
11. *Antonov S.N., Rezvov Yu.G.* // PTE. 2020. No. 6. P. 46. https://doi.org/ 10.31857/S0032816220050262
12. *Gasanov A.R., Gasanov R.A.* // PTE. 2018. No. 3. P.54. https://doi.org/ 10.7868/S0032816218030114
13. *Kotov V.M., Voronko A.I.* // PTE. 2021. No. 4. P.54. https://doi.org/ 10.31857/S0032816221040212
14. *Kotov V.M.* //Avtometriya. 1992. No. 3. P.109.
15. *Antonov S.N.* // ZhTF. 2004. Vol. 74. P. 84. https://doi.org/ 10.1134/1.1809706
16. *Voloshinov V.B., Molchanov V.Ya., Babkina T.M.* //ZhTF. 2000. Vol.70. No. 9. P. 93. https://doi.org/ 10.1134/1.1318107
17. *Anchutkin V.S., Belsky A.B., Voloshinov V.B., Yushkov K.B.* // Optical Journal. 2009. Vol.76. No. 8. P. 29. https://doi.org/ 10.1364/JOT.76.000473
18. *Klochkov V.P., Kozlov L.F., Potykevich I.V., Soskin M.S.* Laser anemometry, remote spectroscopy and interferometry. Handbook. Kiev: Naukova Dumka, 1985.
19. *Koronkevich V.P., Khanov V.A.* Modern laser interferometers. Novosibirsk: Nauka, 1985.
20. *Born M., Wolf E*. Principles of Optics. Moscow: Nauka, 1973.
21. *Fedorov F.I.* Optics of anisotropic media. Moscow: URSS, 2004.
22. *Kotov V.M.* //Acoustical Physics. 2016. Vol. 62. No. 5. P. 525. https://doi.org / 10.7868/S0320791916040109
23. *Zilberman G.E., Kupchenko L.F* // Radio Engineering and Electronics. 1977. Vol. 22. No. 8. P. 1551.
24. *Antonov S.N., Proklov V.V.* // JTP. 1983. Vol. 53. No. 2. P. 306.
25. *Molchanov V.Ya., Kitaev Yu.I., Kolesnikov A.I., Narver V.N., Rozenstein A.Z., Solodovnikov N.P., Shapovalenko K.G.* Theory and Practice of Modern Acousto-optics. Moscow: Publishing House MISiS, 2015.

FIGURE CAPTIONS

Fig. 1. Dependence of phase change δ_m on parameter P for ellipticity values 0.9, 0.8, 0.7, 0.6, 0.5, corresponding to curves *1 – 5*.

Fig. 2. Dependence of rotation angle ψ of the total polarization vector on parameter P. Curves *1 – 5* correspond to the same ellipticities as the curves in Fig. 1.

Fig. 3. Vector diagram of AO-diffraction in uniaxial gyrotropic crystal.

Fig. 4. Photograph of the experimental AO-cell.

Fig. 5. Dependence of the angle ψ of polarization plane rotation (solid curve, left ordinate scale) and ellipticity ρ (dashed curve, right scale) on frequency f of the sound wave.

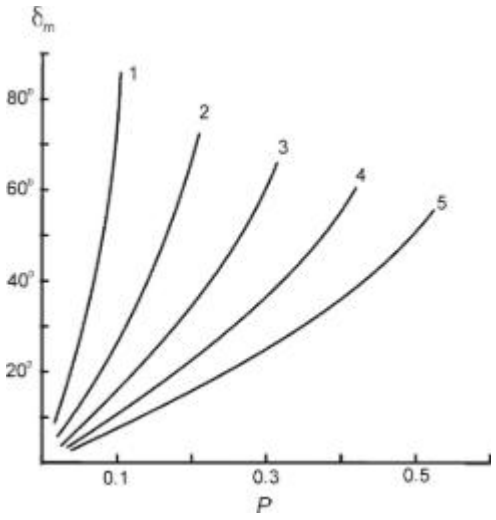

Fig.1.

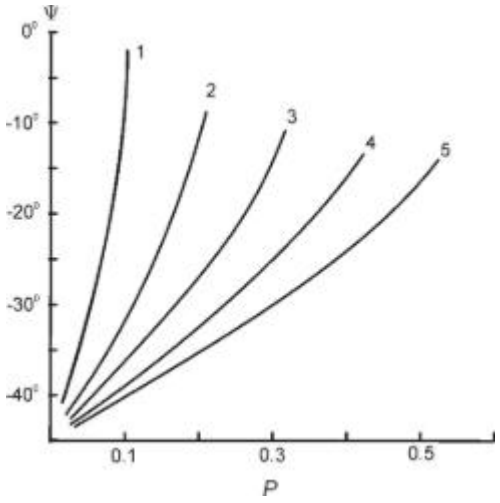

Fig.2.

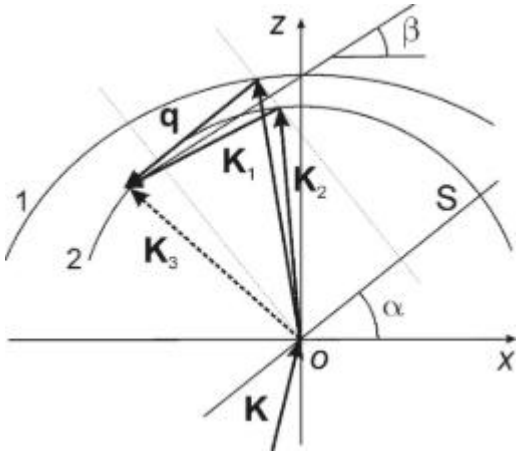

Fig.3.

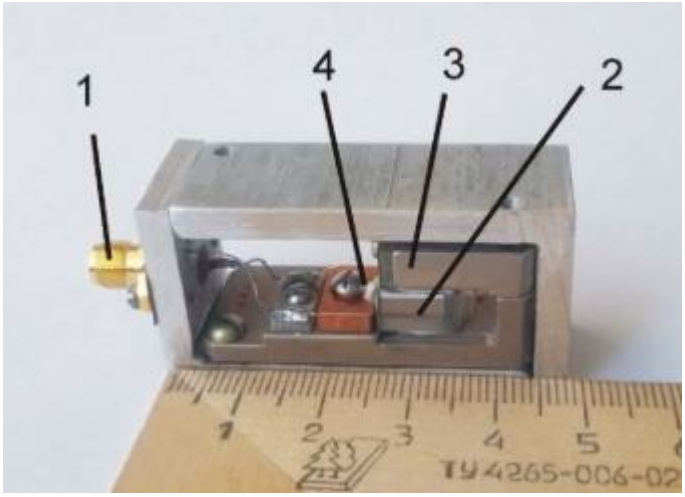

Fig. 4

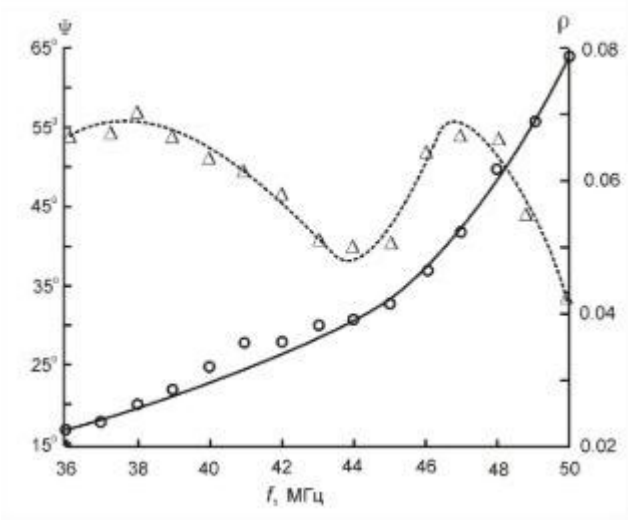

Fig. 5